8
Probing signature of anomalous tcZ coupling through rare B and K decays

8.1 Introduction

In the previous chapters we have been focusing on B-meson decays to probe physics beyond SM. However, apart from the decays of B meson, the top quark decays are particularly important for hunting new physics. As it is the heaviest of all the SM particles, it is expected to feel the effect of NP most. Also, LHC is primarily a top factory producing abundant top quark events. Hence one expects the observation of possible anomalous couplings in the top sector at the LHC. In particular, the FCNC top quark decays, such as $t \to qZ$ $(q = u, c)$, are important as they are highly suppressed within the SM owing to the GIM mechanism. The SM predictions for the branching ratios of $t \to uZ$ and $t \to cZ$ decays are $\sim 10^{-17}$ and 10^{-14}, respectively [233, 234], and are beyond the scope of current detection level at the LHC until new physics enhances their branching ratios up to the present sensitivity of LHC. The present upper bound on the branching ratio of $t \to cZ$ are 2.4×10^{-4} [235] from ATLAS and 4.9×10^{-4} [236] from CMS collaboration at 95% C.L. Thus the observation of any of the FCNC top quark decays at the LHC would imply discovery of new physics.

The possible new physics effects in the top FCNC decays have been incorporated in a model independent way within different theoretical frameworks, see for e.g., [237–251]. In this chapter we investigate the flavour signatures of effective anomalous $t \to cZ$ couplings [144]. The anomalous tcZ couplings can arise in various extensions of the SM. These include universal extra-dimensional model [252], Randall-Sundrum framework of warped extra dimension [253], type-III two-Higgs doublet model [254], and models with vector-like quarks [255]. Apart from enhancing the branching ratio of $t \to cZ$ decay, such couplings would also affect the loop level processes involving the top quark, and hence has the potential to affect rare B and K meson decays via the Z penguin diagrams.

In order to obtain constraints on the anomalous tcZ coupling, we perform a combined fit to (i) all CP conserving observables in $b \to s\mu^+\mu-$ sector, (ii) observables in $b \to se^+e^-$ sector, (iii) the branching ratio of $B^+ \to \pi^+\mu^+\mu^-$ and $B_d \to \mu^+\mu^-$ and (iv) the branching fraction of $K^+ \to \pi^+\,\nu\,\bar{\nu}$. In our analysis we consider the coupling to be real as well as complex. For the complex tcZ coupling, we find that the branching ratio of $t \to c\,Z$ can be as high as 1.91×10^{-4} at 2σ. Then we look for other flavour signatures of this anomalous tcZ coupling. In particular, we examine branching ratio of $K_L \to \pi\,\nu\,\bar{\nu}$ and various CP violating angular observables in $B \to (K, K^*)\,\mu^+\,\mu^-$. We find that the complex tcZ coupling can give rise to large enhancements to various CP violating observables.

The organization of this chapter is as follows. In Sec. 8.2, we describe the effect of tcZ coupling on rare B and K decays. In Sec. 8.3, we discuss about the methodology used in the fit. In Sec. 8.4, we provide fit results along with predictions of various observables. We present our conclusions in Sec. 8.5.

8.2 Effect of anomalous $t \to cZ$ couplings on rare B and K decays

The effective tcZ Lagrangian can be written as [256]

$$\mathcal{L}_{tcZ} = \frac{g}{2\cos\theta_W}\bar{c}\gamma^\mu \left(g_{ct}^L P_L + g_{ct}^R P_R\right) t Z_\mu + \frac{g}{2\cos\theta_W}\bar{c}\frac{i\sigma^{\mu\nu}p_\nu}{M_Z}\left(\kappa_{ct}^L P_L + \kappa_{ct}^R P_R\right) t Z_\mu + \mathrm{h.c.}, \quad (8.1)$$

where $P_{L,R} \equiv (1 \mp \gamma_5)/2$ and $g_{ct}^{L,R}$ and $\kappa_{ct}^{L,R}$ are new physics couplings.

The rare B meson decays induced by the quark level transitions, such as $b \to s\, l^+\, l^-$ and $b \to d\, l^+\, l^-$ along with rare K meson decays induced by the quark level transition, such as $s \to d\nu\bar{\nu}$, occur only at the loop level within the SM and hence are highly suppressed. Within the SM, these processes are dominated by box and Z penguin diagrams. The anomalous tcZ couplings can enter into the Z penguin diagrams, see for e.g., Figs. 8.1 and 8.2, and hence has the potential to affect rare B and K decays. Therefore these decays can be used to constrain anomalous $t \to cZ$ coupling.

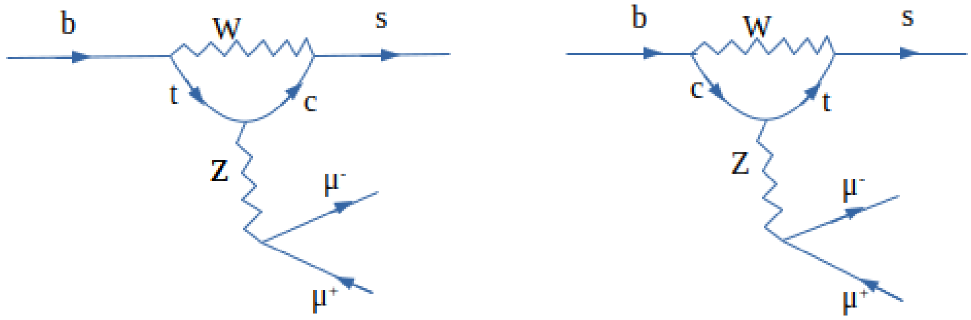

Figure 8.1: Feynman diagrams with the anomalous tcZ coupling contributing to $b \to s\,\mu^+\,\mu^-$ transition.

Let us now consider the contribution of anomalous tcZ couplings to the rare B decays induced by the quark level transition $b \to s\,\mu^+\,\mu^-$. Within the SM, the effective Hamiltonian for the quark-level transition $b \to s\,\mu^+\,\mu^-$ can be written as

$$\mathcal{H}_{SM}(b \to s\,\mu^+\,\mu^-) = -\frac{4G_F}{\sqrt{2}\pi}V_{ts}^* V_{tb}\Big[\sum_{i=1}^{6} C_i(\mu)O_i(\mu) + C_7\frac{e}{16\pi^2}\left[\bar{s}\sigma_{\mu\nu}\left(m_s P_L + m_b P_R\right)b\right]F^{\mu\nu}$$
$$+C_9\frac{\alpha_{em}}{4\pi}\left(\bar{s}\gamma^\mu P_L b\right)\left(\bar{\mu}\gamma_\mu\mu\right) + C_{10}\frac{\alpha_{em}}{4\pi}\left(\bar{s}\gamma^\mu P_L b\right)\left(\bar{\mu}\gamma_\mu\gamma_5\mu\right)\Big], \quad (8.2)$$

where G_F is the Fermi constant, V_{ts} and V_{tb} are the Cabibbo-Kobayashi-Maskawa (CKM) matrix elements and $P_{L,R} = (1 \mp \gamma^5)/2$ are the projection operators. The effect of the operators O_i, $i = 1-6, 8$ can be embedded in the redefined effective Wilson coefficients (WCs) as $C_7(\mu) \to C_7^{\rm eff}(\mu, q^2)$ and $C_9(\mu) \to C_9^{\rm eff}(\mu, q^2)$, where the scale $\mu = m_b$. The form of the operators O_i are given in ref. [150].

The effective tcZ vertices, given in Eq. (8.1), modifies the WCs C_9 and C_{10} through the Z penguin diagrams. There are two such Feynman diagrams, as shown in Fig. 8.1. The contribution from the diagram in the left and right panel is proportional to $V_{tb}V_{cs}^*$ and $V_{cb}V_{ts}^*$, respectively. As $V_{tb}V_{cs}^* \sim \mathcal{O}(1)$ and $V_{cb}V_{ts}^* \sim \mathcal{O}(\lambda^4)$, the dominant contribution comes from the diagram proportional to $V_{tb}V_{cs}^*$ and the contribution from the other diagram can be safely neglected. The new physics contributions to C_9 and C_{10} are given as [246, 247]

$$C_9^{s,NP} = -C_{10}^{s,NP} = -\frac{1}{8\sin^2\theta_W}\frac{V_{cs}^*}{V_{ts}^*}\left[\left(-x_t \ln\frac{M_W^2}{\mu^2} + \frac{3}{2} + x_t - x_t \ln x_t\right) g_{ct}^L\right], \quad (8.3)$$

with $x_t = \bar{m}_t^2/M_W^2$. Here the right handed coupling, g_{ct}^R, is neglected as it is suppressed by a factor of $\bar{m}_c/M_W$. The new physics contributions to $C_{9,10}$ have been calculated in the unitary gauge with the

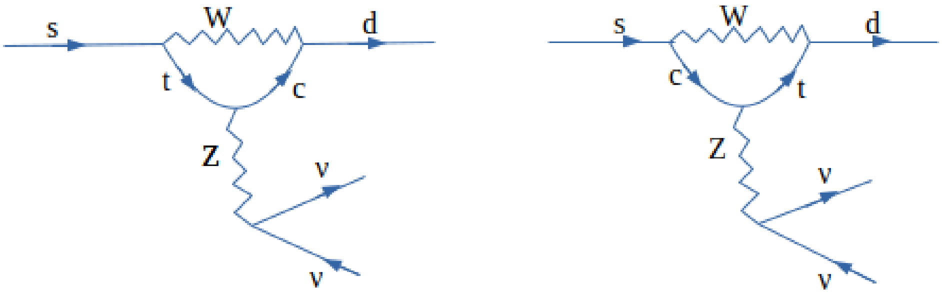

Figure 8.2: Feynman diagrams with the anomalous tcZ coupling contributing to $s \to d\,\nu\,\bar{\nu}$ transition.

modified minimal subtraction ($\overline{\text{MS}}$) scheme [246]. It is found that the new physics tensors operators, defined in the effective Lagrangian Eq. (8.1), do not contribute to $C_{9,\,10}$.

The anomalous tcZ couplings can also contribute to $b \to d\,\mu^+\,\mu^-$ transition via Feynman diagrams shown in Fig. 8.1 with s quark replaced by d quark. Within the SM, the branching ratio for $b \to d\,\mu^+\,\mu^-$ transitions are suppressed relative to $b \to s\,\mu^+\,\mu^-$ processes by the ratio $|V_{td}|^2/|V_{ts}|^2$. The effective Hamiltonian for the process $b \to d\,\mu^+\,\mu^-$ can be obtained from Eq. (8.2) by replacing s by d. The contribution from the diagram on the left panel is CKM suppressed and hence not included in our analysis. The contribution of anomalous tcZ coupling to $b \to d\,\mu^+\,\mu^-$ transition from the other diagram modifies the Wilson coefficients C_9 and C_{10} in the following way

$$C_9^{d,NP} = -C_{10}^{d,NP} = -\frac{1}{8\sin^2\theta_W}\frac{V_{cd}^*}{V_{td}^*}\left[\left(-x_t \ln\frac{M_W^2}{\mu^2} + \frac{3}{2} + x_t - x_t \ln x_t\right) g_{ct}^L\right]. \tag{8.4}$$

Here we have neglected the contributions from right handed coupling, g_{ct}^R, which is suppressed by a factor of $\bar{m}_c/M_W$.

We now consider new physics contribution to $s \to d\,\nu\bar{\nu}$ transition. The anomalous tcZ couplings contributes to $s \to d\,\nu\bar{\nu}$ transition via Feynman diagrams shown in Fig. 8.2. In this case, the CKM contribution from both the diagrams is of the same order, $\mathcal{O}(\lambda^3)$, and hence we include both of them in our analysis. The $K^+ \to \pi^+\,\nu\bar{\nu}$ decay is the only observed decay channel induced by the quark level transition $\bar{s} \to \bar{d}\,\nu\bar{\nu}$. Unlike other K decays, the SM prediction for the branching ratio of $K^+ \to \pi^+\,\nu\bar{\nu}$ is under good control as the long distance contribution to $\mathcal{B}(K^+ \to \pi^+\nu\bar{\nu})$ is about three orders of magnitude smaller than the short-distance contribution [257, 258]. The effective Hamiltonian for $K^+ \to \pi^+\,\nu\bar{\nu}$ in the SM can be written as

$$\mathcal{H}_{eff} = \frac{G_F}{\sqrt{2}}\frac{\alpha}{2\pi\sin^2\theta_W}\sum_{l=e,\mu,\tau}\left[V_{cs}^* V_{cd} X_{NL}^l + V_{ts}^* V_{td} X(x_t)\right] \times (\bar{s}d)_{V-A}(\bar{\nu}_l\nu_l)_{V-A} \tag{8.5}$$

where X_{NL}^l and $X(x_t)$ are the structure functions corresponding to charm and top sector, respectively [150]. The contribution of anomalous tcZ coupling to $\bar{s} \to \bar{d}\,\nu\bar{\nu}$ transition then modifies the structure function $X(x_t)$ in the following way

$$X(x_t) \to X^{\text{tot}}(x_t) = X(x_t) + X^{NP}, \tag{8.6}$$

where

$$X(x_t) = \eta_X \frac{x_t}{8}\left[\frac{2+x_t}{x_t-1} + \frac{3x_t-6}{(1-x_t)^2}\ln x_t\right], \tag{8.7}$$

$$X^{NP} = -\frac{1}{8}\left(\frac{V_{cd}V_{ts}^* + V_{td}V_{cs}^*}{V_{td}V_{ts}^*}\right) \times \left(-x_t \ln\frac{M_W^2}{\mu^2} + \frac{3}{2} + x_t - x_t \ln x_t\right)(g_{ct}^L)^*. \tag{8.8}$$

Here $\eta_x = 0.994$ is the NLO QCD correction factor.

$G_F = 1.16637 \times 10^{-5}$ Gev^{-2}	$\tau_{B_d} = (1.519 \pm 0.007)$ ps
$\sin^2\theta_w = 0.23116$	$\tau_{B^+} = 1.638 \pm 0.004$ ps
$\alpha(M_Z) = \frac{1}{129}$	$f_{B_d} = (190 \pm 1.3)$ MeV [21]
$\alpha_s(M_Z) = 0.1184$	$\kappa_+ = (5.36 \pm 0.026) \times 10^{-11}$ [259]
$m_t(m_t) = 163$ GeV	$\kappa_L = (2.31 \pm 0.01) \times 10^{-10}$
$M_W = 80.385$ GeV	$\lambda = 0.225 \pm 0.001$ [260]
$M_Z = 91.1876$ GeV	$A = 0.826 \pm 0.012$ [260]
$M_{B_d} = 5.27917$ GeV	$\bar{\rho} = 0.148 \pm 0.013$ [260]
$M_{B^+} = 5.27932$ GeV	$\bar{\eta} = 0.348 \pm 0.010$ [260]
$m_\mu = 0.105$ GeV	

Table 8.1: Decay constants, bag parameters, QCD corrections and other parameters used in our analysis. When not explicitly stated, they are taken from the Particle Data Group [210].

8.3 Constraints on the anomalous tcZ couplings

In order to obtain the constraints on the anomalous tcZ coupling g_{ct}^L, we perform a χ^2 fit using all measured observables in B and K sectors. The χ^2 fit is performed using the CERN minimization code `MINUIT` [204]. The total χ^2 is written as a function of two parameters: $\mathrm{Re}(g_{ct}^L)$, and $\mathrm{Im}(g_{ct}^L)$. The χ^2 function is defined as

$$\chi^2_{\text{total}} = \chi^2_{b\to s\,\mu^+\,\mu^-} + \chi^2_{b\to s\,e^+\,e^-} + \chi^2_{b\to d\,\mu^+\,\mu^-} + \chi^2_{s\to d\nu\bar{\nu}} \,. \tag{8.9}$$

In our analysis, χ^2 of an observable A is defined as

$$\chi^2_A = \left(\frac{A - A^c_{exp}}{A^{err}_{exp}}\right)^2 , \tag{8.10}$$

where the measured value of A is $(A^c_{exp} \pm A^{err}_{exp})$.

In the following subsections, we discuss the individual components of the function χ^2_{total}, i.e the χ^2 of different observables which are being used as inputs.

8.3.1 Constraints from $b \to s\,\mu^+\,\mu^-$ sector

As the anomalous tcZ coupling considered in this work does not account for lepton flavour non-universal effects, we do not consider R_K and R_{K^*} measurements in our fits. Instead, we consider all relevant measurements related to $b \to s\,\mu^+\,\mu^-$ and $b \to s\,e^+\,e^-$.

The quark level transition $b \to s\,\mu^+\,\mu^-$ induces inclusive and exclusive semi-leptonic B decays along with the purely leptonic $\bar{B}_s \to \mu^+\mu^-$ decay. In our analysis we include following observables:

1. The branching ratio of $B_s \to \mu^+\mu^-$ which is $(3.1 \pm 0.7) \times 10^{-9}$ [189].
2. The differential branching ratio of $B^0 \to K^{*0}\mu^+\mu^-$ measured in various q^2 bins [261–264].
3. Various angular observables in $B^0 \to K^{*0}\mu^+\mu^-$ [44, 48, 262, 264, 265].
4. The differential branching ratio of $B^+ \to K^{*+}\mu^+\mu^-$ in various q^2 bins [262, 266].
5. The differential branching ratio of $B^0 \to K^0\mu^+\mu^-$ in various q^2 bins [262, 266].
6. The differential branching ratio of $B^+ \to K^+\mu^+\mu^-$ in several q^2 bins [262, 266].

7. The measurements of the angular observables and the differential branching ratio of $B_s^0 \to \phi\mu^+\mu^-$ [43].

8. The experimental measurements for the differential branching ratio of $B \to X_s\mu^+\mu^-$ [226].

In the context of anomalous tcZ couplings, the WCs are related as $C_9^{s,NP} = -C_{10}^{s,NP}$. Hence we can use the above $b \to s\mu^+\mu^-$ observables to obtain constraints on the coupling g_{ct}^L using Eq. (8.3).

The χ^2 function for all $b \to s\mu^+\mu^-$ observables listed above is defined as

$$\chi^2_{b\to s\,\mu^+\,\mu^-} = (O_{th}(C_i) - O_{exp})^T\,\mathcal{C}^{-1}\,(O_{th}(C_i) - O_{exp}) \tag{8.11}$$

where $O_{th}(C_i)$ are the theoretical predictions of $b \to s\mu^+\mu^-$ observables which are calculated using `flavio` [228] and O_{exp} are the corresponding experimental measurements. The total covariance matrix $\mathcal{C}$ is obtained by adding the individual theoretical and experimental covariance matrices.

8.3.2 Constraints from $b \to s\,e^+\,e^-$ sector

The following measurements, mediated by $b \to s\,e^+\,e^-$ transitions, are taken into fit:

1. Angular observables P_4' and P_5' in $B \to K^*\,e^+\,e^-$, both in two q^2 bins $[1, 6]$ and $[14.18, 19]$ GeV^2 [227].

2. The branching ratio of $B^0 \to K^*\,e^+\,e^-$ in $[0.001, 1]$ GeV^2 bin [224].

3. The branching ratio of $B^+ \to K^+\,e^+\,e^-$ in [1,6] GeV^2 bin [49].

4. The K^* polarization fraction in $B^0 \to K^*\,e^+\,e^-$ [225].

5. The branching fractions of $B \to X_s\,e^+\,e^-$ within two q^2 bins $[1, 6]$ and $[14.2, 25]$ GeV^2 [226].

The constraints coming from $B_s \to e^+\,e^-$ is weak as the current upper bound on its branching ratio [189] is about seven orders of magnitude away from the SM prediction. Although this is not included directly in our fit, we have checked that the fit results do not evade the upper limit. The χ^2 function for the set of observables in $b \to s\,e^+\,e^-$ transition is defined as

$$\chi^2_{b\to s\,e^+\,e^-} = \sum \frac{\left(O_i^{th} - O_i^{exp}\right)^2}{\sigma_{O_i}^{th\,2} + \sigma_{O_i}^{exp\,2}}, \tag{8.12}$$

where $\sigma_{O_i}^{th}$ and $\sigma_{O_i}^{exp}$ are the SM and experimental uncertainties in each observable.

8.3.3 Constraints from $b \to d\,\mu^+\,\mu^-$ sector

The quark level transition $b \to d\mu^+\,\mu^-$ gives rise to inclusive semi-leptonic decay $\bar{B} \to X_d\,\mu^+\,\mu^-$ and exclusive semi-leptonic decay such as $\bar{B} \to (\pi^0,\,\rho)\,\mu^+\,\mu^-$. However, so far, none of these decays have been observed. We only have an upper bound on their branching ratios [267, 268]. However, LHCb has observed the $B^+ \to \pi^+\,\mu^+\,\mu^-$ decay, which is induced by $b \to d\mu^+\,\mu^-$ transition, with measured branching ratio of $(2.3 \pm 0.6 \pm 0.1) \times 10^{-8}$ [269]. This is the first measurement of any decay channel in $b \to d\,\mu^+\,\mu^-$ sector.

The theoretical expression for $\mathcal{B}(B^+ \to \pi^+\,\mu^+\,\mu^-)$ in the presence of anomalous tcZ coupling can be obtained from Ref. [270] by replacing the WCs $C_{9,\,10}$ by that given in Eq. (8.4). The contribution to $\chi^2_{\rm total}$ is

$$\chi^2_{B^+\to\pi^+\,\mu^+\,\mu^-} = \Big(\frac{\mathcal{B}(B^+ \to \pi^+\,\mu^+\,\mu^-) - 2.3 \times 10^{-8}}{0.66 \times 10^{-8}}\Big)^2, \tag{8.13}$$

where, following ref. [270], a theoretical error of 15% is included in $\mathcal{B}(B^+ \to \pi^+\,\mu^+\,\mu^-)$. This error is mainly due to uncertainties in the $B^+ \to \pi^+$ form factors [161].

We also include the constraint from $B_d \to \mu^+\mu^-$ decay. The branching ratio of $B_d \to \mu^+\,\mu^-$ in the presence of anomalous tcZ coupling is given by

$$\mathcal{B}(B_d \to \mu^+\,\mu^-) = \frac{G_F^2\alpha^2 M_{B_d} m_\mu^2 f_{B_d}^2 \tau_{B_d}}{16\pi^3}|V_{td}V_{tb}^*|^2 \times \sqrt{1-4(m_\mu^2/M_{B_d}^2)}\,\left|C_{10}+C_{10}^{d,NP}\right|^2 . \quad (8.14)$$

In order to include $\mathcal{B}(B_d \to \mu^+\,\mu^-)$ in the fit, we define

$$B_{\rm lepd} = \frac{16\pi^3\mathcal{B}(B_d \to \mu^+\,\mu^-)}{G_F^2\alpha^2 M_{B_d} m_\mu^2 f_{B_d}^2 \tau_{B_d}|V_{td}V_{tb}^*|^2\sqrt{1-4(m_\mu^2/M_{B_d}^2)}} . \quad (8.15)$$

Using the inputs given in Table 8.1 and $\mathcal{B}(B_d \to \mu^+\,\mu^-)_{\rm exp} = (3.9 \pm 1.6) \times 10^{-10}$ [189] , we get

$$B_{\rm lepd,exp} = 60.83 \pm 25.18. \quad (8.16)$$

The contribution to χ^2 from $\mathcal{B}(B_d \to \mu^+\,\mu^-)$ is then

$$\chi^2_{B_d\to\mu^+\mu^-} = \Big(\frac{B_{\rm lepd}-60.83}{25.18}\Big)^2 . \quad (8.17)$$

Thus we have,

$$\chi^2_{b\to d\,\mu^+\,\mu^-} = \chi^2_{B^+\to\pi^+\,\mu^+\,\mu^-} + \chi^2_{B_d\to\mu^+\mu^-} . \quad (8.18)$$

8.3.4 Constraints from $s \to d\,\nu\bar\nu$ sector

The branching ratio of $K^+ \to \pi^+\nu\bar\nu$, the only measurement in this sector, in the presence of anomalous tcZ coupling is given by

$$\frac{\mathcal{B}(K^+ \to \pi^+\nu\bar\nu)}{\kappa_+} = \left(\frac{{\rm Re}(V_{cd}V_{cs}^*)}{\lambda}P_c(X) + \frac{{\rm Re}(V_{td}V_{ts}^*)}{\lambda^5}X^{\rm tot}(x_t)\right)^2 + \left(\frac{{\rm Im}(V_{td}V_{ts}^*)}{\lambda^5}X^{\rm tot}(x_t)\right)^2 , \quad (8.19)$$

where $P_c(X) = 0.38 \pm 0.04$ [271] is the NNLO QCD corrected structure function in the charm sector and

$$\kappa_+ = r_{K^+}\frac{3\alpha^2\mathcal{B}(K^+ \to \pi^0 e^+\nu)}{2\pi^2\sin^4\theta_W}\lambda^8 . \quad (8.20)$$

Here $r_{K^+} = 0.901$ encapsulates the isospin-breaking corrections in relating the branching ratio of $K^+ \to \pi^+\nu\bar\nu$ to that of the well-measured decay $K^+ \to \pi^0 e^+\nu$. $X^{\rm tot}(x_t)$ is given in Eq. (8.6). With inputs used in Table 8.1 and $\mathcal{B}(K^+ \to \pi^+\nu\bar\nu)_{\rm exp}$, we estimate

$$\frac{\mathcal{B}(K^+ \to \pi^+\nu\bar\nu)}{\kappa_+} = 3.17 \pm 2.05 , \quad (8.21)$$

In order to include $\mathcal{B}(K^+ \to \pi^+\nu\bar\nu)$ in the fit, we define

$$\chi^2_{K^+\to\pi^+\nu\bar\nu} = \Big(\frac{\mathcal{B}(K^+ \to \pi^+\nu\bar\nu)/\kappa_+ - 3.17}{2.05}\Big)^2 + \Big(\frac{P_c(X)-0.38}{0.04}\Big)^2. \quad (8.22)$$

Thus, the error on $P_c(X)$ has been taken into account by considering it to be a parameter and adding a contribution to $\chi^2_{\rm total}$.

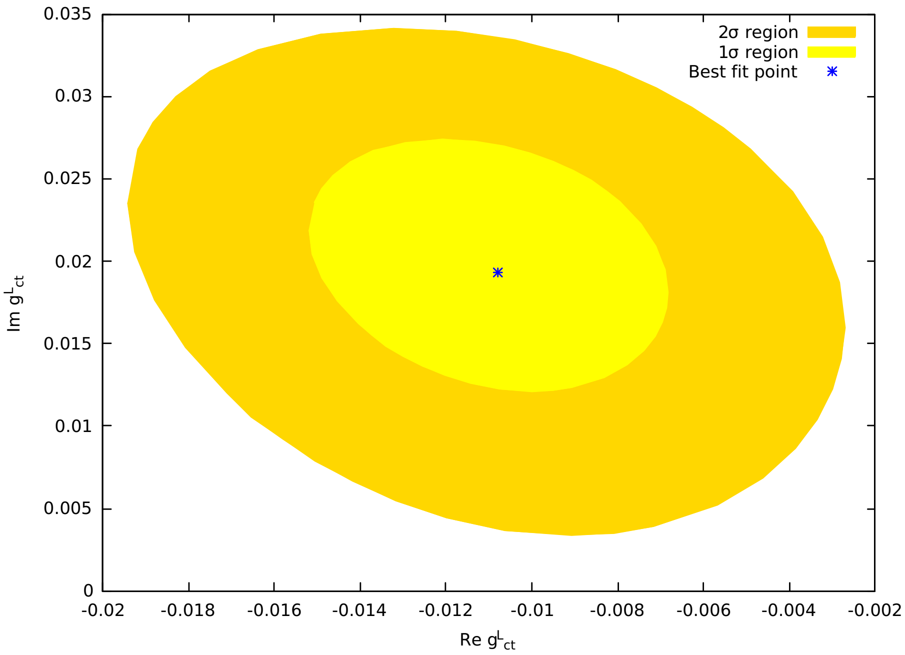

Figure 8.3: Allowed parameter space for the complex tcZ coupling.

Real coupling	Complex coupling
$g_{ct}^L = (-6.51 \pm 1.46) \times 10^{-3}$	$\mathrm{Re}(g_{ct}^L) = (-1.02 \pm 0.38) \times 10^{-2}$; $\mathrm{Im}(g_{ct}^L) = (1.79 \pm 0.84) \times 10^{-2}$

Table 8.2: Values of anomalous tcZ couplings.

8.4 Results and discussions

The fit results for real and complex tcZ couplings are presented in Table 8.2. The allowed 1 and 2σ parameter space for the complex tcZ coupling is presented in Fig.8.3.

8.4.1 $\mathcal{B}(t \to c\,Z)$

The branching ratio of $t \to cZ$ is defined as [238, 272, 273]

$$\mathcal{B}(t \to c\,Z) = \frac{\Gamma(t \to cZ)}{\Gamma(t \to bW)}, \tag{8.23}$$

where, the leading-order (LO) decay width of $t \to bW$ is given as [274]

$$\Gamma(t \to bW) = \frac{G_F m_t^3}{8\sqrt{2}\pi} |V_{tb}|^2 \beta_W^4 (3 - 2\beta_W^2), \tag{8.24}$$

with $\beta_W = (1 - m_W^2/m_t^2)^{1/2}$, being the velocity of the W boson in the top quark rest frame. On the other hand, the LO decay width of $t \to cZ$ can be written as [238, 272, 273]

$$\Gamma(t \to cZ) = \frac{G_F m_t^3}{8\sqrt{2}\pi} \frac{|g_{ct}^L|^2 + |g_{ct}^R|^2}{2} \beta_Z^4 (3 - 2\beta_Z^2), \tag{8.25}$$

where $\beta_Z = (1 - m_Z^2/m_t^2)^{1/2}$, the velocity of the Z boson in the top quark rest frame.

Using the fit results, we find that for real tcZ coupling, $\mathcal{B}(t \to c\,Z) = (7.73 \pm 3.47) \times 10^{-6}$ and the 2σ upper bound is 1.47×10^{-5}. For complex tcZ coupling, the branching ratio of $t \to c\,Z$ is $(7.75 \pm 5.67) \times 10^{-5}$ and the 2σ upper bound on the branching ratio is 1.91×10^{-4} which could be measured at the LHC. In fact this is very close to the present upper bound from ATLAS [235] and CMS [236] collaborations. The ATLAS collaboration reported the upper limit to be 2.4×10^{-4} at 95% C.L. using the data collected at a center of mass energy of 13 TeV. The CMS collaboration set the upper limit at 4.9×10^{-4} at 95% C.L. using the data recorded at a center of mass energy of 8 TeV. Thus the observation of $t \to cZ$ at the level of 10^{-4} would not only be an indication of anomalous tcZ coupling but could also imply that these couplings are complex. If such tcZ complex couplings are present then it should also show its presence in other decays. In the following we study the impact of this coupling on various CP-violating observables related to the rare decays of K and B mesons. It would be interesting to see whether large deviations are possible in some of these observables.

8.4.2 $\mathcal{B}(K_L \to \pi^0\,\nu\,\bar{\nu})$

The branching ratio of $K_L \to \pi^0\,\nu\,\bar{\nu}$ is a purely CP violating quantity, i.e., it vanishes if CP is conserved. The SM branching ratio is predicted to be $(2.90 \pm 0.40) \times 10^{-11}$. As this process is highly suppressed in the SM, it is sensitive to new physics. The preset upper bound set by KOTO experiment at J-PARC on $\mathcal{B}(K_L \to \pi^0\,\nu\,\bar{\nu})$ is 3.0×10^{-9} [275] at 90% C.L. which is about three orders of magnitude above the SM prediction. This result improves the previous upper limit [276, 277] by an order of magnitude. This experiment should have enough data for the first observation of the decay by about 2021.

Within the SM, $K_L \to \pi^0\,\nu\,\bar{\nu}$ decay is dominated by loop diagrams with top quark exchange. Hence anomalous tcZ coupling can modify its branching ratio. The branching ratio of $K_L \to \pi^0\,\nu\,\bar{\nu}$ in the presence of tcZ coupling is given by

$$\mathcal{B}(K_L \to \pi^0\,\nu\,\bar{\nu}) = \kappa_L \left[\frac{\mathrm{Im}\left(V_{ts}^* V_{td} X^{\mathrm{tot}}(x_t)\right)}{\lambda^5}\right]^2, \tag{8.26}$$

where $X^{\mathrm{tot}}(x_t)$ is given in Eq. (8.6).

Using fit result for the complex tcZ coupling, we get $\mathcal{B}(K_L \to \pi^0 \nu\bar{\nu}) = (8.83 \pm 4.68) \times 10^{-11}$. The 2σ upper bound on $\mathcal{B}(K_L \to \pi^0\,\nu\,\bar{\nu})$ is obtained to be $\leq 1.82 \times 10^{-10}$. Thus the anomalous tcZ couplings can provide an order of magnitude enhancement in the branching ratio of $K_L \to \pi^0\,\nu\,\bar{\nu}$.

8.4.3 CP violating observables in $B \to (K^*,\, K)\,\mu^+\,\mu^-$

Within the SM, the CP violating observables in $b \to s\,\mu^+\,\mu^-$ are highly suppressed. The complex tcZ coupling can give rise to additional phase for CP violation, which can affect several CP violating observables in $b \to s\,\mu^+\,\mu^-$ sector. Here, we study various CP violating observables in $B \to (K^*,\, K)\,\mu^+\,\mu^-$ decays in the presence of complex anomalous tcZ couplings. The four fold angular distribution of the decay $\bar{B}^0 \to \bar{K}^{*0}(K^-\pi^+)\mu\mu$ can be described by the kinematical variables q^2, θ_K, θ_l and ϕ [203]

$$\frac{d^4\Gamma(\bar{B}^0 \to \bar{K}^{*0}(K\pi)\mu\mu)}{dq^2\, d\cos\theta_l\, d\cos\theta_K\, d\phi} = \frac{9}{32\pi} I(q^2, \theta_l, \theta_K, \phi), \tag{8.27}$$

where

$$\begin{aligned} I(q^2, \theta_l, \theta_K, \phi) = {} & I_1^s \sin^2\theta_K + I_1^c \cos^2\theta_K + (I_2 s \sin^2\theta_K + I_2^c \cos^2\theta_K)\cos 2\theta_l + I_3 \sin^2\theta_K \sin^2\theta_l \cos 2\phi \\ & + I_4 \sin 2\theta_K \sin 2\theta_l \cos\phi + I_5 \sin 2\theta_K \sin\theta_l \cos\phi + (I_6^s \sin^2\theta_K + I_6^c \cos^2\theta_K)\cos\theta_l \\ & + I_7 \sin 2\theta_K \sin\theta_l \sin\phi + I_8 \sin 2\theta_K \sin 2\theta_l \sin\phi + I_9 \sin^2\theta_K \sin^2\theta_l \sin 2\phi. \end{aligned} \tag{8.28}$$

The corresponding full angular distribution of the CP-conjugate decay $B^0 \to K^{*0}(K^+\pi^-)\mu\mu$ can be obtained by replacing the angular coefficients $I_{1,2,3,4,7} \to \bar{I}_{1,2,3,4,7}$ and $I_{5,6,8,9} \to -\bar{I}_{5,6,8,9}$ in Eq. (8.27) and $\bar{I}_i$ is equal to I_i with all weak phase conjugated.

The CP-violating observables are defined as

$$A_i = \frac{I_i - \bar{I}_i}{d(\Gamma + \bar{\Gamma})/dq^2} \tag{8.29}$$

These asymmetries are largely suppressed in SM because of the small weak phase of CKM and hence they are sensitive to complex new physics couplings. These symmetries can get significant contribution from the new physics in the presence of CP-violating phase [198, 278, 279]. The direct CP asymmetries for $B \to (K, K^*)\,\mu^+\,\mu^-$ decays can be measured at the level of few percent at the LHCb [280–282]. Measurement of other CP violating observables would require higher statistics which can be achieved at HL-LHC [283]. Along with the LHCb measurements, the predictions for CP violating asymmetries A_i in

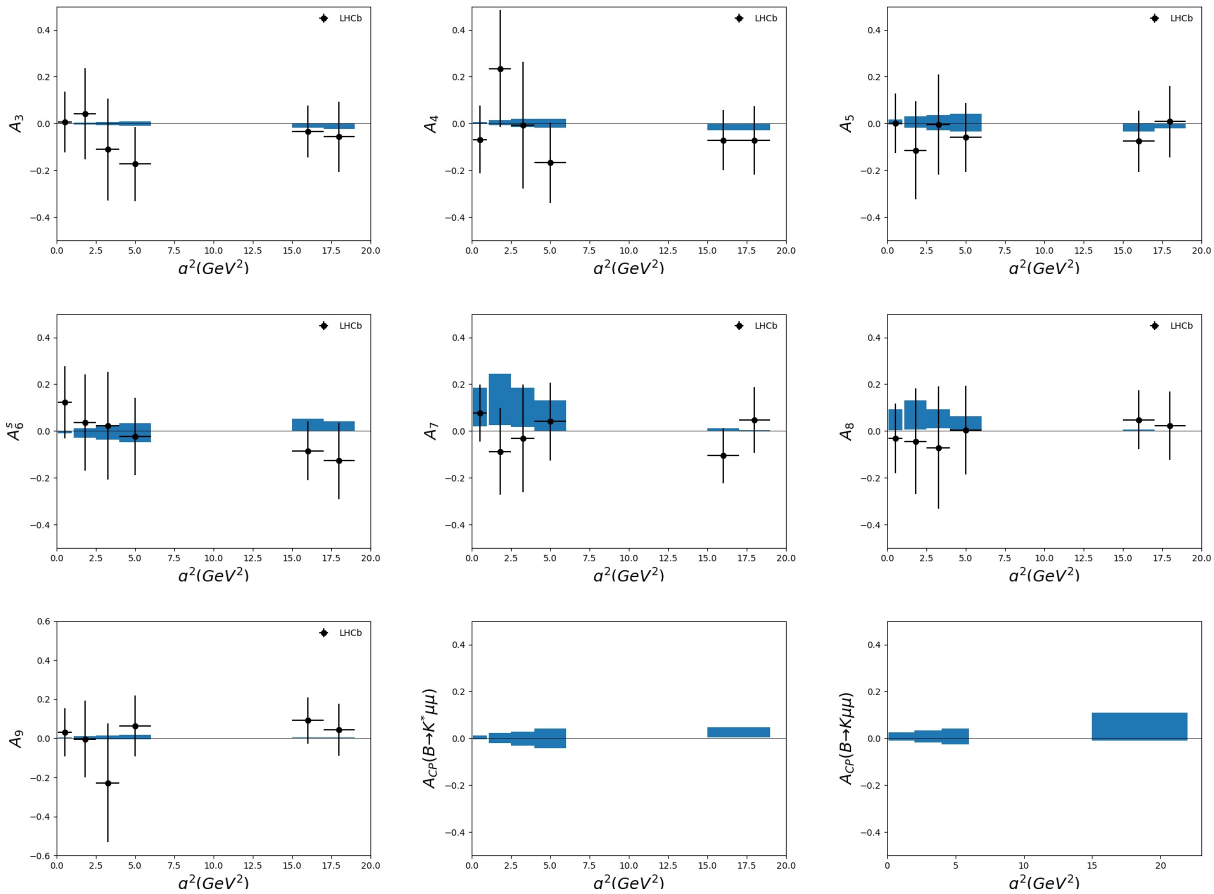

Figure 8.4: (Color Online) The plots depicts various CP violating observables in $B \to (K^*,\, K)\,\mu^+\,\mu^-$ decays as a function of q^2.

the presence of complex anomalous tcZ couplings are shown in fig. 8.4. In ref. [229], it was shown that the asymmetries A_3 and A_9 are very sensitive to the chirally flipped operators. In the present scenario, there is no chirally flipped operator contribution and hence large enhancement is not expected in these asymmetries. This can also be seen from our results. The asymmetry A_7 can be enhanced up to 20% whereas enhancement in A_8 can be up to 10% in the low-q^2 region. We also find that large entrancement is not possible the direct-CP asymmetries in $B \to K\mu^+\mu^-$ and $B \to K^*\mu^+\mu^-$.

8.5 Conclusions

The FCNC decays of top quark are considered as a reliable probe to physics beyond SM. Although these transitions are highly suppressed in the SM, but the promising new physics contributions can enhance them to the observation level of current collider experiments. In this chapter, we study the flavour signatures of effective anomalous $t \to cZ$ couplings. We use all relevant measurements in B and K meson systems to constrain the new physics parameter space by considering both real and complex tcZ couplings. Finally, we provide predictions for the branching ratio of $t \to cZ$ along with branching ratio of $K_L \to \pi^0 \nu\bar{\nu}$ and various CP violating obervables in $B \to (K, K^*)\mu^+\mu^-$ decays. Our finding are as follows:

- For real tcZ coupling, the 2σ upper bound on the branching ratio of $t \to cZ$ is 1.47×10^{-5}, whereas that for the complex coupling is 1.91×10^{-4}. The current experimental upper bound on the branching ratio of $t \to cZ$ is 2.4×10^{-4}. Hence, any future measurement of this branching ratio at the level of 10^{-4} would imply the coupling to be complex.

- The complex tcZ coupling provide an interesting signature in the case of CP violating decay $K_L \to \pi^0 \nu\bar{\nu}$. We find that the 2σ upper bound on the branching ratio of this decay is 1.82×10^{-10}, an order of magnitude higher than its SM prediction.

- The complex tcZ couplings can provide large enhancements in various CP violating observables in $B \to K^* \mu^+ \mu^-$ decay.